

Recombinant Differential Anchorage Probes that Tower over the Spatial Dimension of Intracellular Signals for High Content Screening and Analysis

Laura Schembri,[†] Marion Zanese,[‡] Gaelle Depierre-Plinet,[‡] Muriel Petit,[‡] Assia Elkaoukabi-Chaibi,[‡] Loic Tauzin,[‡] Cristina Florean,^{†,§} Lydia Lartigue,[†] Chantal Medina,[†] Christophe Rey,[†] Francis Belloc,^{||} Josy Reiffers,[†] François Ichas,^{†,‡} and Francesca De Giorgi^{*,†,‡}

INSERM U916, Institut Bergonié, Université Victor Segalen, 229 cours de l'Argonne, 33076 Bordeaux, France, FLUOFARMA, 2 rue Robert Escarpit, 33600 Pessac, France, Dipartimento delle Scienze Biomediche Sperimentali, Università di Padova, 35121 Padova, Italia, and CHU de Bordeaux, Hôpital du Haut Lévêque, 33600 Pessac, France

Recombinant fluorescent probes allow the detection of molecular events inside living cells. Many of them exploit the intracellular space to provide positional signals and, thus, require detection by single cell imaging. We describe here a novel strategy based on probes capable of encoding the spatial dimension of intracellular signals into “all-or-none” fluorescence intensity changes (differential anchorage probes, DAPs). The resulting signals can be acquired in single cells at high throughput by automated flow cytometry, (i) bypassing image acquisition and analysis, (ii) providing a direct quantitative readout, and (iii) allowing the exploration of large experimental series. We illustrate our purpose with DAPs for Bax and the effector caspases 3 and 7, which are key players in apoptotic cell death, and show applications in basic research, high content multiplexed library screening, compound characterization, and drug profiling.

Fluorescent-protein biosensors are useful tools for monitoring molecular events in live cells, such as protein translocation, enzyme activation, protein–protein interaction, and the operation of second messengers.^{1,2} The generic design of fluorescent biosensors is based on the development of chimeric constructs capable of undergoing conditional changes in spectra or intensity that report the event of interest. This is generally obtained by genetic modification of the emitting protein or by the construction of fluorescence resonance energy transfer (FRET) probes.¹ However, spectral-based signals can be difficult to acquire, and this often restricts the application of these probes to single cell and single parameter studies in basic research.

Recently, the interest for fluorescent protein biosensors propagated to the drug discovery field with the emergence of high-

throughput cell imaging platforms³ designed to screen large libraries of compounds or of targeted siRNAs. A new generation of positional probes based on changes in intracellular distribution was developed and implemented in cell-based high-content screening (HCS) assays running on these platforms.³ However, this technology is objectively limited by the need of specific equipment for high-resolution image acquisition and analysis that significantly complicates the screen and exponentially increases the equipment costs as well as the amount of image data to process.^{4,5}

In this study, we describe an alternative approach allowing one to perform HCS assays by flow cytometry with a new class of simple fluorescent probes capable of converting positional signals into intensity responses. This method is based on the differential retention of a fluorescent recombinant probe following plasma membrane permeabilization (coined “differential anchorage probes”, DAPs) and is capable of detecting a variety of molecular events such as proteolytic activities and changes in intracellular compartmentalization.

We present here two specific DAPs targeting key molecular steps in apoptotic pathway: namely, Bax activation and caspase 3 or 7 activity. With these probes, we successfully quantified the target molecular events at high throughput and multiplexed their detection with other parameters like cell cycle status, proliferation index, or cytolysis. Our results show that DAPs constitute a robust alternative tool for quantitative and high content identification/characterization of molecular targets, as well as for drug discovery.

EXPERIMENTAL SECTION

Plasmids. The cDNA encoding for GFP-Bax was a gift of R.J. Youle. The cDNA encoding the mom-C3/7 DAP was generated by insertion of the DEVD coding sequence by site-directed mutagenesis on the GFP-RR cDNA (kindly provided by Nica Borgese) with a Quick Change Site-directed mutagenesis kit (Stratagene). The DEVD -mom TMD sequence was cloned in pCopGreen, pTURBOGFP, and pHcRed-tandem plasmids (Evro-

* Corresponding author. Address: INSERM U916, Institut Bergonié, 229 cours de l'Argonne, 33076 Bordeaux, France. Tel: +33 (0)556330433. Fax: +33 (0)556333206. E-mail: francesca.degiorgi-ichas@inserm.fr.

[†] Université Victor Segalen.

[‡] FLUOFARMA.

[§] Università di Padova.

^{||} Hôpital du Haut Lévêque.

(1) Zhang, J.; Campbell, R. E.; Ting, A. Y.; Tsien, R. Y. *Nat. Rev. Mol. Cell. Biol.* 2002, 3, 906–918.

(2) Giepmans, B. N. G.; Adams, S. R.; Ellisman, M. H.; Tsien, R. Y. *Science* 2006, 312, 217–224.

(3) Lang, P.; Yeow, K.; Nichols, A.; Scheer, A. *Nat. Rev. Drug Discovery* 2006, 5, 343–356.

(4) Baatz, M.; Arini, N.; Schäpe, A.; Binnig, G.; Linssen, B. *Cytometry, Part A* 2006, 69, 652–658.

(5) Gribbon, P.; Sewing, A. *Drug Discovery Today* 2003, 8, 1035–1043.

gen). For pm-C3/7 DAP, the cDNA of the plasma membrane anchor domain was synthesized by polymerase chain reaction (PCR) corresponding to the 80–136 aa fragment of murine SNAP-25 and cloned into mom-C3/7 DAP by substituting the cb5 TM domain. For nu-C3/7 DAP, the DEVD coding sequence was generated by site-directed mutagenesis of GFP-H2B cDNA (Pharmingen) with the Quick Change Site-directed mutagenesis kit (Stratagene). For mis-C3/7 DAP, the ANT2 cDNA was amplified by PCR and cloned into the mom-C3/7 DAP vector as replacement to the mom TM domain.

Cell Culture and Transfection. All cell lines were maintained at 37 °C in Dulbecco's MEM medium (Gibco, Life Technologies) supplemented with 10% fetal calf serum in a humidified atmosphere of 5% CO₂/95% air.

For plasmid transfection, cells were plated directly on 24 well or 96 well plates or on 25 mm diameter round glass coverslips (according to the considered experiment) and transiently transfected when reaching 50% of confluence using Exgen 500, as described in the manufacturer's instructions (Euromedex). For siRNA transfection, cells were seeded in 96 well plates (10 000 cells/well) and transfected 24 h later with 100nM siRNA from a triplicate <> CMGC kinases >> bank (Ambion) using siPORTLipid (Ambion). Bank details are provided in the supplementary Table 1 in the Supporting Information. For the generation of cell clones stably expressing DAPs, transfected cells were selected 72 h after transfection by adding Geneticin to the culture medium (G418-Promega). Western Blotting cells (1×10^6) were washed in PBS and scraped on ice in 300 μL of lysis buffer supplemented with protease inhibitors. Cells were incubated for 2 h at 4 °C under stirring and centrifuged for 15 min at 10 000 rpm and 4 °C. Proteins from supernatant were dosed and electrophoresed in 12% sodium dodecyl sulfate-polyacrylamide gel electrophoresis (SDS-PAGE) gel. The proteins were transferred to Hybond C nitrocellulose (Amersham) and western-blotted using antimyc (Santa Cruz). Signal was detected using ECL (Amersham).

Immunostaining. Cells were fixed in 3.7% formaldehyde for 20 min at room temperature before permeabilization in 0.1% triton. Aspecific binding was blocked by incubation in 0.2% gelatin/PBS, and staining was performed using specific primary antibodies against anticytochrome c (clone 6H2.B4; Pharmingen). After washing, cells were incubated with the appropriate antiTexasRed-conjugated secondary antibodies (Molecular Probes).

Microscopy, Image Analysis. Living or fixed immunostained cells were observed using either a Zeiss Axiovert 100 M inverted motorized microscope coupled with a Micromax 1300YHS 5 MHz cooled CCD camera (Princeton Instruments) or a LSM 510 Meta confocal microscope. Acquisition and image processing were performed using Metamorph 4.5 (Universal Imaging) or the LSM image analysis software (Carl Zeiss).

DAP Assays. Transiently transfected or stably DAP expressing cells were detached by trypsin and resuspended in an intracellular saline solution (130 mM KCl, 10 mM NaCl, 20 mM 4-(2-hydroxyethyl)-1-piperazineethanesulfonic acid (HEPES), 1 mM MgSO₄, 5 mM succinate pH 7.2) supplemented with 50 μM digitonin, 50 μM ethylene glycol tetraacetic acid (EGTA), and 4% of fetal calf serum. The cell samples were analyzed by flow cytometry (488 nm laser) (Partec PAS, Becton Dickinson Facs-

Calibur HTS, Beckman Coulter FC500). GFP or CopGreen fluorescence was detected in FL1.

Assay Z'determination was performed according to ref 21, using in each plate eight control wells (solvent-treated) and eight wells treated with 2 μM staurosporine (24 h and 48 h exposure runs).

Multiplexed Assays. DAP Plus Cytolysis. Before permeabilization, cells were incubated on ice with a saline solution supplemented with 0.5 μg/mL ethidium monoazide bromide (EMA) (Molecular Probes) for 10 min and exposed to a white light for 15 min. Then, cells were rinsed, detached, and treated as above. EMA fluorescence was detected in FL3.

DAP Plus Cell Cycle. Propidium iodide (50 μg/mL, Sigma) was added to the permeabilization solution, and after 5 min at room temperature, the cells were incubated 1 h at 4 °C. PI signal was detected in FL3.

DAP Plus Proliferation Index. Prior to seeding, the cells were incubated at 37 °C in a solution of 0.3 M glucose and 5 μM DiI (1,1'-dioctadecyl-3,3',3'-tetramethylindocyanine perchlorate) for 15 min under mild stirring. The cells were then rinsed twice, counted, and seeded onto 96 well plates. A sample of cells was measured (FL3 channel) to obtain the day 0 value. The proliferation index was determined by the ratio of the median value of DiI signal at day 0 and of the median value of DiI signal at day 2 or day 3 of treatment.

RESULTS AND DISCUSSION

GFP-Bax Chimera is a DAP Detecting Bax Activation. The proapoptotic protein Bax plays a central role in the mitochondrial phase of apoptosis and is considered a potential target in the development of new apoptosis-based therapies.⁶ Bax is “silent”, soluble at rest, and relocates from the cytosol to the mitochondrial outer membrane (MOM) upon activation. This intracellular relocalization coincides with a change of Bax solubility due to the unfolding and insertion of one or more protein domains into the MOM. This “activatable anchorage” is pivotal for its proapoptotic function.^{7,8}

To obtain a quantification of Bax activation by flow cytometry, we developed a new, yet simple, approach based on the differential retention of the resting and activated forms of the protein following selective plasma membrane permeabilization (PMP): in preapoptotic cells, soluble cytosolic GFP-Bax (resting) rapidly diffused out of the cell collapsing the fluorescence signal; while in apoptotic ones, membrane inserted GFP-Bax (activated) was unaffected by PMP and the fluorescence signal was retained (Figure 1A,B).

In a cell clone (clone 10) stably expressing GFP-Bax, the fluorescent chimera appeared to act as a reliable reporter of Bax relocalization to the MOM. Using PMP, we are able to precisely quantify, in each experimental condition, the percentage of cells in which Bax activation took place (Figure 1C). The dose-response and the time-course functions of apoptosis induced by staurospo-

(6) Walensky, L. D.; Kung, A. L.; Escher, I.; Malia, T. J.; Barbuto, S.; Wright, R. D.; Wagner, G.; Verdine, G. L.; Korsmeyer, S. J. *Science* **2004**, *305*, 1466–1470.

(7) De Giorgi, F.; Lartigue, L.; Bauer, M. K. A.; Schubert, A.; Grimm, S.; Hanson, G. T.; Remington, S. J.; Youle, R. J.; Ichas, F. *FASEB J.* **2002**, *16*, 607–609.

(8) Zhu, Y.; Liu, X.; Hildeman, D.; Peyerl, F. W.; White, J.; Kushnir, E.; Kappler, J.; Marrack, P. *J. Exp. Med.* **2006**, *203*, 1147–1152.

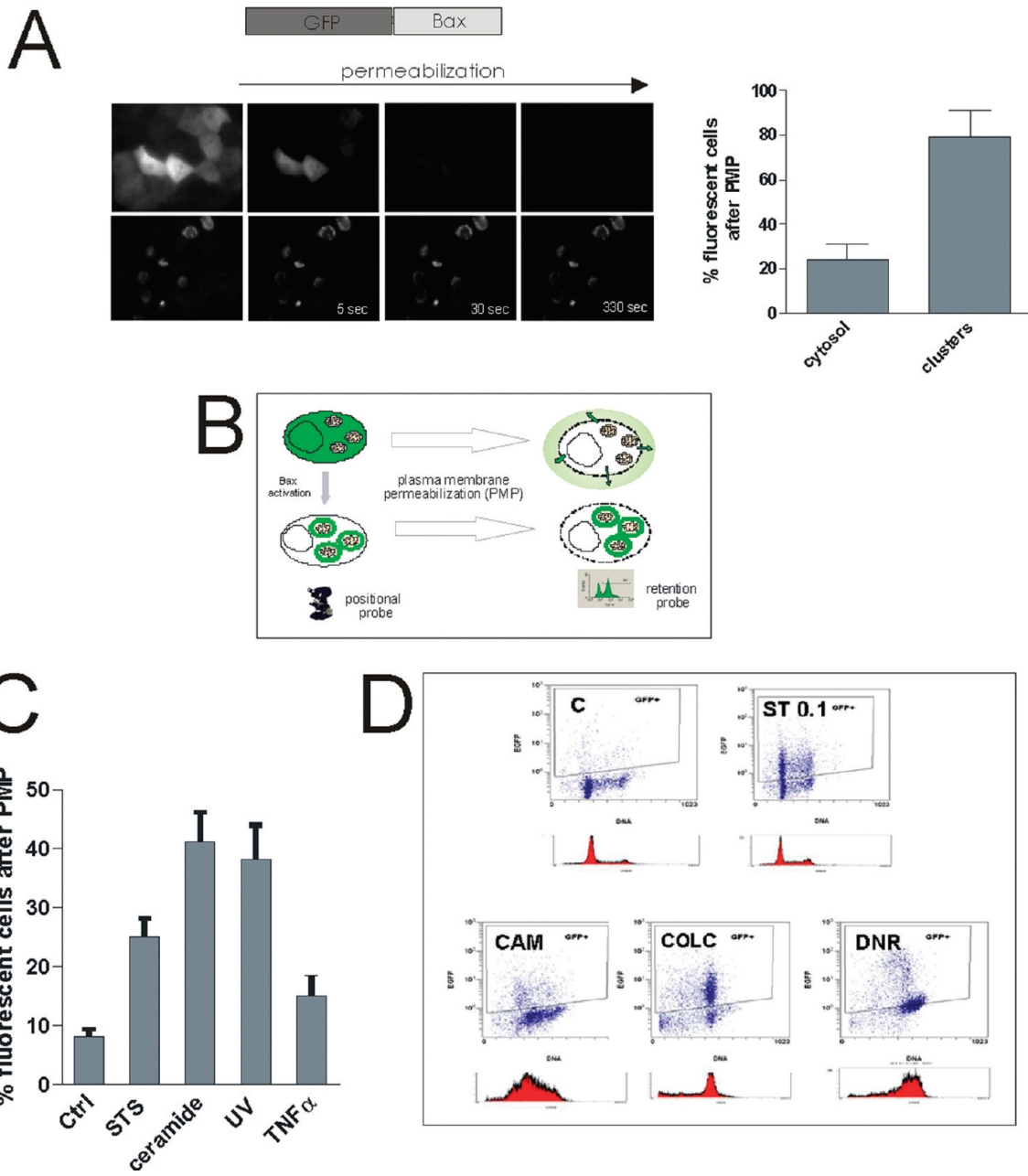


Figure 1. Conversion of a positional signal by plasma membrane permeabilization (PMP): Bax as a natural DAP. (A) Imaging of HeLa cells expressing GFP-Bax treated (lower sequence) or not (upper sequence) with STS ($1 \mu\text{M}$, 3 h). At rest, GFP-Bax is cytosolic (top left), and PMP (digitonin $50 \mu\text{M}$) releases GFP-Bax. In STS-treated cells, activated GFP-Bax assumes a clustered distribution (bottom left) that resist PMP. Right-hand histogram: post-PMP fluorescence retention in cells exhibiting either resting GFP-Bax (cytosol, $n = 15$) or activated GFP-Bax (clusters, $n = 20$). Digitonin was added to living cells during a confocal microscopy time-lapse experiment, and quantification of the fluorescent signal loss in regions, respectively, placed on cytosolic/nuclear compartment and on mitochondrial clusters was performed using Metamorph. (B) Schematic representation of the Bax DAP assay principle. (C) Bax DAP assay by flow cytometry of a HeLa clone expressing GFP-Bax (clone 10) treated 24 h with proapoptotic agents. (D) Multiplex of Bax DAP assay with cell cycle analysis. Bax activation can be restricted to specific cell cycle phases: G0-G1 with Camptothecin, G2 M phase with Colcemid, and S phase with Daunorubicin. Bax activation is cell cycle independent with STS.

rine (STS) showed that the quantification of Bax activation by DAP coincided with the appearance of a mitochondrial depolarization, a phenotypic marker of apoptosis (Figure S-1a,b in the Supporting Information).

Moreover, the Bax DAP assay could easily be multiplexed with cell cycle analysis monitored by propidium iodide (PI) staining after PMP (Figure 1D). Clone 10 cells were treated with STS, camptothecine, colcemide, or daunorubicine. All these compounds induce Bax activation and, except for STS, an arrest in specific phases of the

cell cycle: S/G2 for camptothecine and G2/M for colcemide and daunorubicine. The multiplexed detection of Bax and cell cycle revealed a strong cell cycle dependence of Bax activation by the topoisomerase poisons. In camptothecin treated cells, Bax was mainly activated in phase G1 while the cells were blocked in S/G2/M. In the case of daunorubicin, Bax was mainly activated in phase S while the cells were blocked in G2/M (Figure 1D).

DAPs for Protease Detection. As a mirror image of the Bax DAP, we reasoned that DAPs could represent an interesting

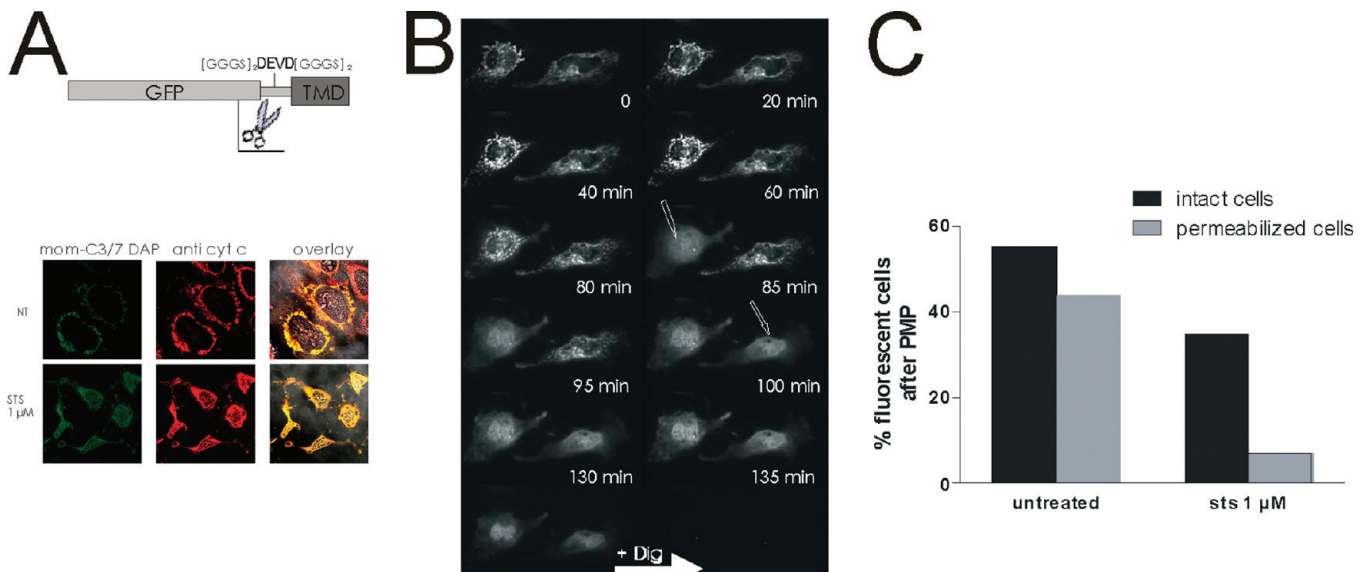


Figure 2. Artificial DAP sensing proteases: a caspase 3/7 probe. (A) Confocal images of control and STS-treated HeLa cells ($1 \mu\text{M}$, 6 h) expressing the caspase 3/7 sensor “mom-C3/7 DAP” (GFP green) and immunostained for cytochrome c (red) show that GFP and cytochrome c are released during apoptosis. (B) Imaging of STS-treated HeLa cells expressing mom-C3/7 DAP. At the single cell level, caspase 3 and 7 activation is “all-or-none” and takes place within 5 min. Last frame: PMP clears the cytosolic GFP signal in cells with activated caspase 3/7. (C) Flow cytometry of mom-C3/7 DAP in transiently transfected HeLa cells treated with STS ($1 \mu\text{M}$, 8 h). Cleavage of the mom-C3/7 DAP by caspase 3/7 is revealed by PMP.

strategy to measure intracellular proteolytic activities which induce the cleavage of membrane proteins and the release of soluble fragments into the cytosol. Some proteins like APP, the substrate of γ -secretase, which is central in the pathogenesis of Alzheimer’s disease, naturally behave as a DAP, since the proteolytic event releases a soluble fragment from a membrane protein, as we showed in a previous work.⁹

Thus, we reasoned that this approach could be extended to other protease substrates by designing specific fluorescent probes (i) artificially anchored to subcellular compartments (ii) that could be specifically released to the cytosolic phase by the protease of interest.

During execution of apoptosis, intracellular proteases named caspases are activated and orchestrate the degradation of the intracellular contents.¹⁰ Caspase 3 and 7 are the principal effectors of apoptotic cell death, and their activity constitutes a specific marker of this process,¹¹ which is deregulated in many tumors, and therefore represents a candidate target for new anticancer drugs.¹²

To obtain a DAP monitoring caspase 3 or 7 activity in live cells, we fused GFP to a mitochondrial outer membrane (mom) anchor domain¹³ through a synthetic linker containing the consensus site for caspase 3 and 7:DEVD (Figure 2A). This chimeric construct (mom-C3/7 DAP) localized at the mitochondrial surface (Figure 2A,B) with the fluorescent moiety exposed in the cytosol.¹³ Live HeLa cells expressing mom-C3/7 DAP were imaged by time lapse fluorescence microscopy and challenged with $1 \mu\text{M}$ STS

(Figure 2B and Figure S-2 in the Supporting Information). After 85 min for the first cell and 100 min for the second, a release of the mom-C3/7 DAP signal from mitochondria to the cytosol took place and completed in less than 3 min, resulting in a total disappearance of any mitochondrial signal anchorage. This change of intracellular distribution, which makes the fluorescent signal sensitive to PMP (Figure 2B), corresponds to the cleavage of the DAP by caspases, as confirmed by a Western blot analysis of STS treated cells (Figure S-2 in the Supporting Information). In addition, immunofluorescence staining of endogenous cytochrome c revealed that the cytosolic distribution of the probe coincided with the release of cytochrome c from mitochondria, showing that probe redistribution specifically took place in apoptotic cells (Figure 2A).

This DAP could be detected by flow cytometry as well: the percentage of GFP positive cells upon PMP provided a direct readout of the caspase 3 or 7 activation in HeLa cells transiently transfected with mom-C3/7 DAP (Figure 2C). Thus, combination of DAPs with PMP can reveal intracellular molecular events that have a spatial component to analytical instruments devoid of spatial discrimination.

Exploring Anchorage Strategies for DAPs. Since DAP assays require an anchorage of the fluorescent probe to a membrane or an intracellular compartment, we tested the possible interest of the use of alternative anchorage strategies by developing new C3/7 DAPs addressed to different subcellular compartments.

SNAP-25 belongs to the SNARE family that is involved in the vesicle secretion process and localizes to the plasma membrane due to the palmitoylation of four cysteines.¹⁴ Thus, in order to target C3/C7 DAP to the plasma membrane, we fused the GFP-DEVD moiety of the previous probe to the 80–136 domain of SNAP-25 which is responsible for the membrane anchorage of

- (9) Florean, C.; Zampese, E.; Zanese, M.; Brunello, L.; Ichas, F.; De Giorgi, F.; Pizzo, P. *Biochim. Biophys. Acta* **2008**, *1783* (8), 1551–60.
- (10) Fischer, U.; Jänicke, R. U.; Schulze-Osthoff, K. *Cell Death Differ.* **2003**, *10*, 76–100.
- (11) Vaculova, A.; Zhivotovsky, B. *Methods Enzymol.* **2008**, *442*, 157–81.
- (12) Beauparlant, P.; Shore, G. C. *Curr. Opin. Drug Discovery Dev.* **2003**, *6*, 179–187.
- (13) Borgese, N.; Gazzoni, I.; Barberi, M.; Colombo, S.; Pedrazzini, E. *Mol. Biol. Cell* **2001**, *12*, 2482–2496.

- (14) Montecucco, C.; Schiavo, G.; Pantano, S. *Trends Biochem. Sci.* **2005**, *30*, 367–372.

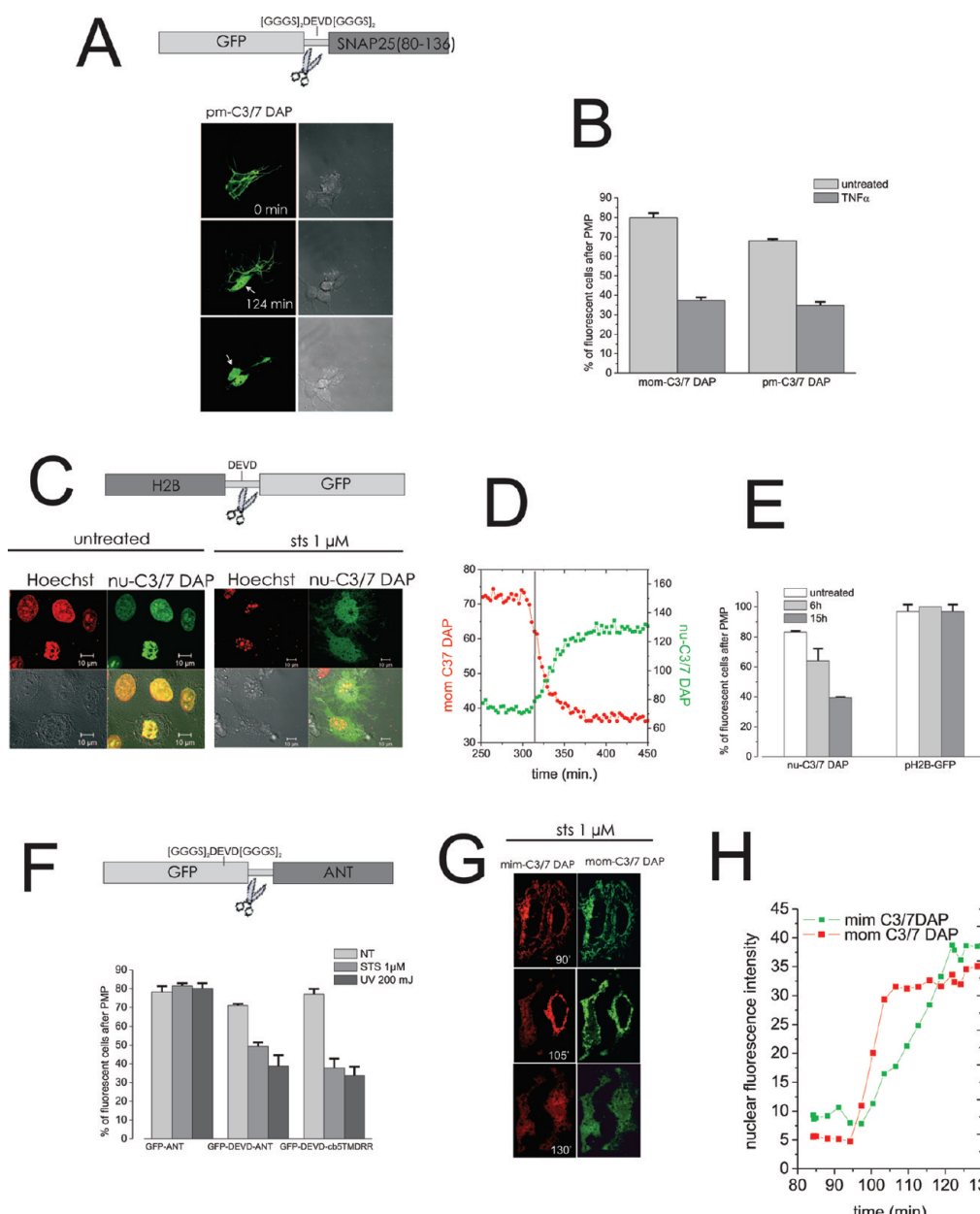


Figure 3. Anchoring C3/7 DAPs to different subcellular structures. (A) SHSY-5Y cells expressing pm-C3/C7 DAP treated with 1 μ M STS show signal redistribution from plasma membrane to cytosol. (B) Flow cytometry of HeLa cells reveals that mom-C3/C7 DAP and pm-C3/C7 DAP respond simultaneously (TNF α 10 ng/mL + cycloheximide (CHX) 10 μ M, 3 h). (C) HeLa cells expressing nu-C3/C7 DAP show a nuclear to cytosol fluorescence redistribution after STS challenge (1 μ M, 3 h). (D) Simultaneous detection of nu-C3/C7 DAP (GFP green) and mom-C3/C7 DAP (HcRed red) in a single HeLa cell shows a short response lag of the two probes, indicating rapid DEVDase activity diffusion. (E) Flow cytometry of nu-C3/C7 DAP in HeLa cells treated with STS confirms that response of the DAP depends on the DEVD linker. (F) Flow cytometry of HeLa cells expressing mis-C3/C7 DAP, mom-C3/C7 DAP, or a simple GFP-ANT2 fusion (mis-GFP) show that the two C3/C7 DAPs behave similarly and depend on DEVD. (G) Simultaneous detection of mis-C3/C7 DAP (GFP) and mom-C3/C7 DAP (HcRed) in single HeLa cells. After STS, the response of mom-C3/C7 DAP precedes mis-C3/C7 DAP (left-hand cell at 105 min). (H) Quantification confirms that mis-C3/C7 DAP is cleaved second to mom-C3/C7 DAP.

the protein¹⁵ (Figure 3A). At rest, this new fusion protein behaved as a topological marker of the plasma membrane in HeLa, SHSY-5Y, and Jurkat cells and was resistant to PMP. Similarly to mom-C3/C7 DAP, pm-C3-DAP allowed the detection of C3/7 activity by imaging (Figure 3A) and by flow cytometry (Figure 3B). The multiplexed detection of both probes by time-lapse confocal microscopy in HeLa cells challenged with STS revealed that the

building up of DEVDase activity was simultaneous at the plasma membrane and at the mitochondrial surface (not shown).

To sense DEVDase activity within the nucleus, the fluorescent probe was anchored to the nucleoplasm by fusion with the entire histone 2B protein (H2B).¹⁶ H2B-GFP remains associated to DNA even in apoptotic cells where its fluorescent signal stains the picnotic nuclei and resists PMP (Figure S-3 in the Supporting

(15) Gonzalo, S.; Greentree, W. K.; Linder, M. E. *J. Biol. Chem.* **1999**, *274*, 21313–21318.

(16) Kanda, T.; Sullivan, K. F.; Wahl, G. M. *Curr. Biol.* **1998**, *8*, 377–385.

Information and Figure 3C). The nuclear C3/7 DAP (nu-C3/7 DAP) was obtained by inserting the DEVD sequence between H2B and GFP. This construct stained the nuclei in healthy cells, but in this case, its signal became diffuse in the apoptotic ones (Figure 3C). This indicated that active caspase 3 or 7 had gained access to the nuclear compartment allowing GFP to detach and to leak out into the cytosol (Figure 3C,D). After PMP, free GFP was washed out, allowing quantification of the percentage of cells with nuclear DEVDase activity by flow cytometry (Figure 3E).

It is tempting to speculate that DAPs could be used to detect events at restricted subcellular locations or interfaces. This property could, for instance, be used to spatially beacon a proteolytic activity. Using single cell imaging, we analyzed the differential rise of DEVDase activity in the cytosol and in the nucleus by recording simultaneously mom-C3/7DAP and nu-C3/7 DAP. We observed that there was a very short, but not statistically significant, lag between the response of the two probes, compatible with the notion that once activated, caspase 3 and/or 7 does not encounter a real barrier during its diffusion throughout the cell (Figure 3D).

Finally, we constructed a DAP to evaluate the diffusion of caspase 3 and 7 from the cytosol to the mitochondrial intermembrane space (MIS) where it gains access to one of its important substrates: the respiratory chain complex I.¹⁷ To this aim, we used the adenine translocator (ANT2) as anchoring moiety. GFP-DEVD was fused to the N-ter of ANT2 that protrudes in the MIS (mis-C3/7 DAP; Figure 3F).¹⁸ The fluorescence protease protection assay¹⁹ of mis-C3/7 DAP in control cells confirmed the correct sorting of the probe to the MIS (not shown). However, second to apoptosis induction by STS or UV exposure, cleavage of mis-C3-DAP occurred, indicating that DEVDase activity could be directly detected in this subcellular compartment (Figure 3F–H). Whether detection of this activity in the MIS is due to the onset of a permeability of the MOM, to cytosolic caspase 3 or 7,¹⁷ or to an in situ activation of pro-caspase 3 or 7 remains to be elucidated.

DAPs for a High Content Pharmacological Characterization of Drugs in Different Cell Type Backgrounds. C3/C7 DAPs constitute a simple and robust tool to evaluate caspase 3 and 7 activity by flow cytometry and only require a rudimentary cell sample preparation protocol. We, thus, generated a series of 10 cell clones stably transfected and expressing mom-C3/7DAP, derived from 10 different human tumor cell lines: HeLa (cervix carcinoma), HCT116 (colon carcinoma), DU145 and DU145 RC0.1 (prostate carcinoma), HuH7 (hepatoma), MCF7 (breast carcinoma), SHSY-5Y (neuroblastoma), HL60 (promyelocytic leukemia), HT29 (colon carcinoma), LNCaP (prostate cancer). Figure 4A shows a row cytometric readout of the HeLa cell clone in control and single dose STS-treated conditions and the quantification gate used to titrate the percentage of cells exhibiting DEVDase activity. Figure 4B shows the full dose response functions obtained for staurosporine and etoposide in the 10 different cell clones. In each cell type, this new high content approach was quantitative enough to allow a pharmacological

characterization of the tested compounds (Figure 4D) with a clear determination of the affinity (EC50) and efficacy (maximal response) in the different tumor cell backgrounds (Figure 4D). This small panel of cell clones can easily be used to compare proapoptotic drugs one to another or to classify them, note for instance that the proapoptotic activity of etoposide is much more dependent on the tumor cell type background than STS.

Multiplexing: Target Identification and Drug Discovery.

We found that DAP assays were robust enough to be multiplexed with the simultaneous detection of other parameters of interest and that such assays could be completely managed by a fully automated platform. In first instance, we concentrated on assays combining the simultaneous detection of caspase 3/7 activity with other key cellular parameters like cell proliferation, cell cycle progression, and loss of plasma membrane integrity (cytolysis) to screen genetic or compound libraries. We achieved a comprehensive automation of the multiplexed assay “C3/7 DAP plus proliferation” based on mom-C3/7 DAP and the cell proliferation probe Dil²⁰ in a 96 well format. We used 24 and 48 h test compound exposures on the HeLa cell clone stably expressing mom-C3/7 DAP, with a screening throughput of 200 test conditions per hour, and with an integration of 2000 single cell measurements per test condition. With such settings, the automated assay yielded a Z' factor²¹ of 0.837 for the 24 h exposure series and of 0.909 for a 48 h exposure (see Experimental Section).

This multiplexed approach allows the rapid and functional identification of targets possibly relevant for the treatment of cancer, by screening siRNA libraries designed to suppress targets of interest. We processed three independent libraries of synthetic siRNA targeting a group of 59 cellular protein kinases involved in cell cycle control (see supplementary Table 1 in the Supporting Information) with a multiplexed screen based on mom-C3/7 DAP and the cell proliferation probe Dil. For each targeted kinase, we gathered 2000 single cell measurements and obtained (i) a quantification of the proapoptotic effect of its suppression by detecting the percentage of cells with activated caspase 3/7 and (ii) a quantification of the cytostatic effect of the suppression by deriving a proliferation index from the individual cell Dil measurements. In Figure 5A, the multiplexed representation of the screening results yields a bidimensional map that allows a clear distinction of the siRNAs which have a mere cytostatic effect from those which lead to apoptosis. These results provide insight on the cellular role played by the targeted kinases, allowing the rapid identification of “essential” targets that once suppressed not only cause a proliferation arrest but also trigger apoptosis.

The same approach can be applied to chemical libraries in order to differentiate apoptosis inducers from pure cytostatic agents at the level of a primary screening.

In Figure 4B, a test library of molecules was used to validate the assay for a single dose screening (10 μM, 24 h exposure). We included, in the test library, antineoplastic drugs commonly used in the clinical management of cancer such as camptothecine, docetaxel, etoposide, vincristine, and proapoptotic compounds like STS and brefeldine A. Figure 4B shows that the high content primary screen was capable of directly sorting the cytostatic and

(17) Ricci, J.; Gottlieb, R. A.; Green, D. R. *J. Cell Biol.* 2003, 160, 65–75.

(18) Pebay-Peyroula, E.; Dahout-Gonzalez, C.; Kahn, R.; Trézéguit, V.; Lauquin, G. J.; Brandolin, G. *Nature* 2003, 426, 39–44.

(19) Lorenz, H.; Hailey, D. W.; Lippincott-Schwartz, J. *Nat. Methods* 2006, 3, 205–210.

(20) Hitoshi, Y.; Gururaja, T.; Pearsall, D. M.; Lang, W.; Sharma, P.; Huang, B.; Catalano, S. M.; McLaughlin, J.; Pali, E.; Peelle, B.; et al. *Chem. Biol.* 2003, 10, 975–987.

(21) Zhang, J.; Chung, T.; Oldenburg, K. *J. Biomol. Screening* 1999, 4, 67–73.

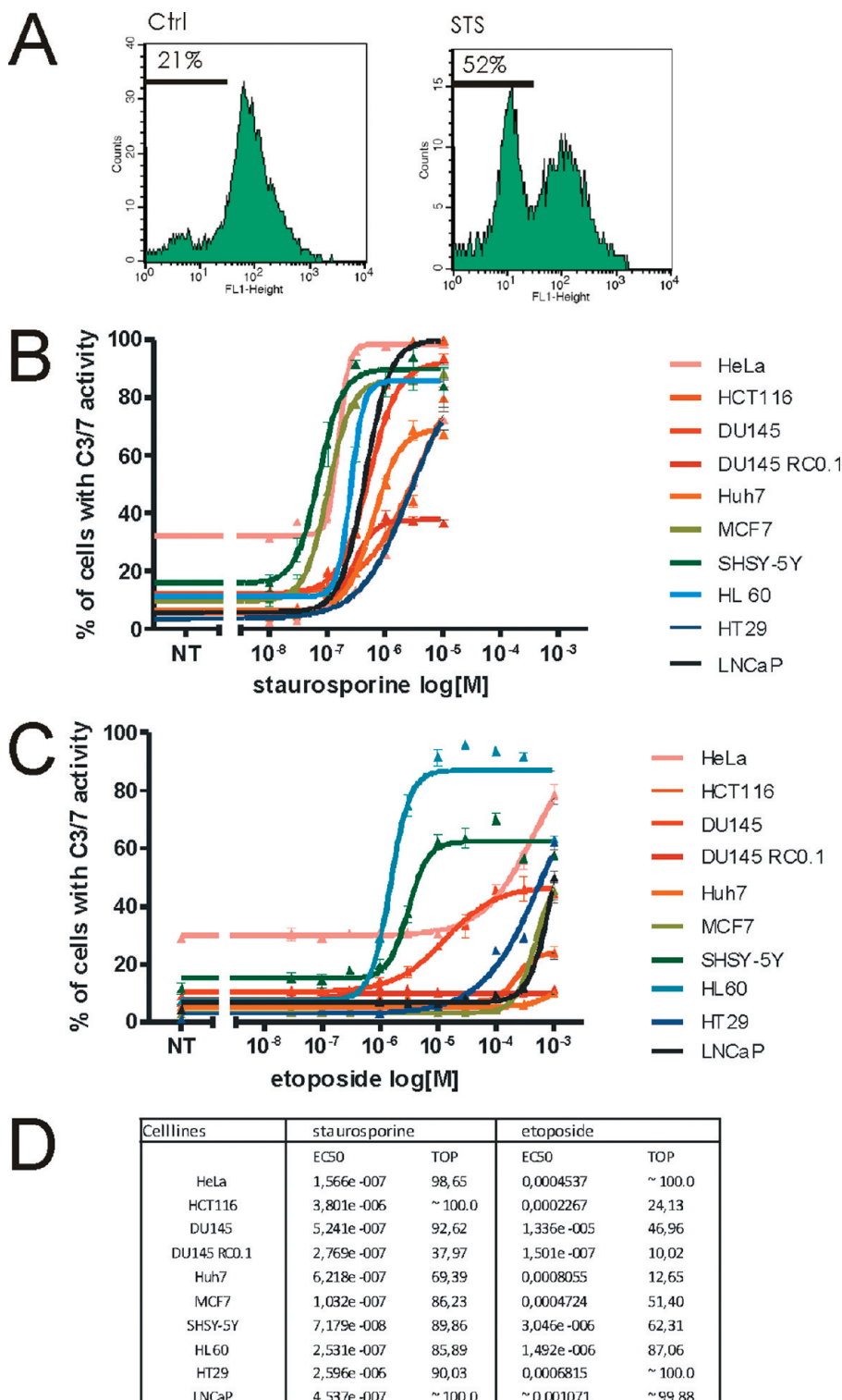


Figure 4. DAPs for a high content pharmacological characterization of drugs in different cell types. (A) Quantification of percentage of cells with caspase 3 and 7 activity by flow cytometry in a HeLa cell stable clone stably expressing mom-C3/7DAP in control and single dose STS-treated conditions. (B, C) Dose response functions obtained for staurosporine (B) and etoposide (C) in 10 cell clones stably expressing mom-C3/7DAP, derived from different human tumor cell lines: HeLa (cervix carcinoma), HCT116 (colon carcinoma), DU145 and DU145 RC0.1 (prostate carcinoma), Huh7 (hepatoma), MCF7 (breast carcinoma), SHSY-5Y (neuroblastoma), HL60 (promyelocytic leukemia), HT29 (colon carcinoma), LNCaP (prostate cancer). (D) Determination of the affinity (EC50) and efficacy (maximal response) in the different tumor cell lines.

proapoptotic compounds. Once selected as hits, the test compounds can be further characterized using the very same multiplexed assay through the generation of “simultaneous” dose–response functions on caspase 3/7 activity and proliferation.

We show the cases of etoposide, camptothecine, and docetaxel (Figure 5C). The two topoisomerase inhibitors (etoposide, camptothecine) are endowed with very different EC50, respectively, to their ability to inhibit proliferation (low EC50) and to elicit caspase

1	Untransfected	21	CLK3	41	MAPK12
2	ALS2CR7	22	CLK4	42	MAPK13
3	CCRK	23	CRK7	43	MAPK14
4	CDC2	24	DYRK1A	44	MAPK4
5	CDC2L5	25	DYRK1B	45	MAPK6
6	CDK10	26	DYRK2	46	MAPK7
7	CDK2	27	DYRK3	47	MAPK8
8	CDK3	28	DYRK4	48	MAPK9
9	CDK4	29	ERK8	49	Nbak2
10	CDK5	30	FJ3281B	50	PCTK1
11	CDK6	31	GSK3A	51	PCTK2
12	CDK7	32	GSK3B	52	PFTK1
13	CDK8	33	HIPK2	53	PPRF4B
14	CDK9	34	HIPK3	54	RAGE
15	CDKL1	35	ICK	55	SRPK1
16	CDKL2	36	LOC51701	56	STK23
17	CDKL3	37	MAK	57	SRPK2
18	CDKL5	38	MAPK1	58	CDK11
19	CLK1	39	MAPK10	59	C-MYC
20	CLK2	40	MAPK11		

1	4-hydroxy TEMPO	25	Thapsigargin
2	EGTA	26	Bongkrekic acid
3	Gentamycin	27	Cyclosporin A
4	chloramphenicol	28	SB 203580
5	tetracycline HCl	29	Nicotine
6	IPG	30	Nicardipin
7	EUK 8	31	sodium selenite
8	Histamine	32	Ethanol
9	Tocopherol	33	DMSO
10	ampicillin	34	Forskolin
11	kanamycin sulfate	35	Doxorubicin
12	Etoposide	36	Vincristine
13	Brefeldin A	37	Staurosporine
14	Cisplatin	38	Rotenone
15	G418	39	CCCP
16	boric acid	40	Antimycin A
17	succinic acid	41	Purvalanol A
18	BSA fraction V	42	Deguelin
19	camptothecin	43	Okaide acid
20	cycloheximide	44	Fostriecin
21	docetaxel	45	Isopropanol
22	verapamil	46	Calyculin A
23	cytosine arabinoside	47	superfas ligand
24	HA14-1 (BTB02933)	48	NT

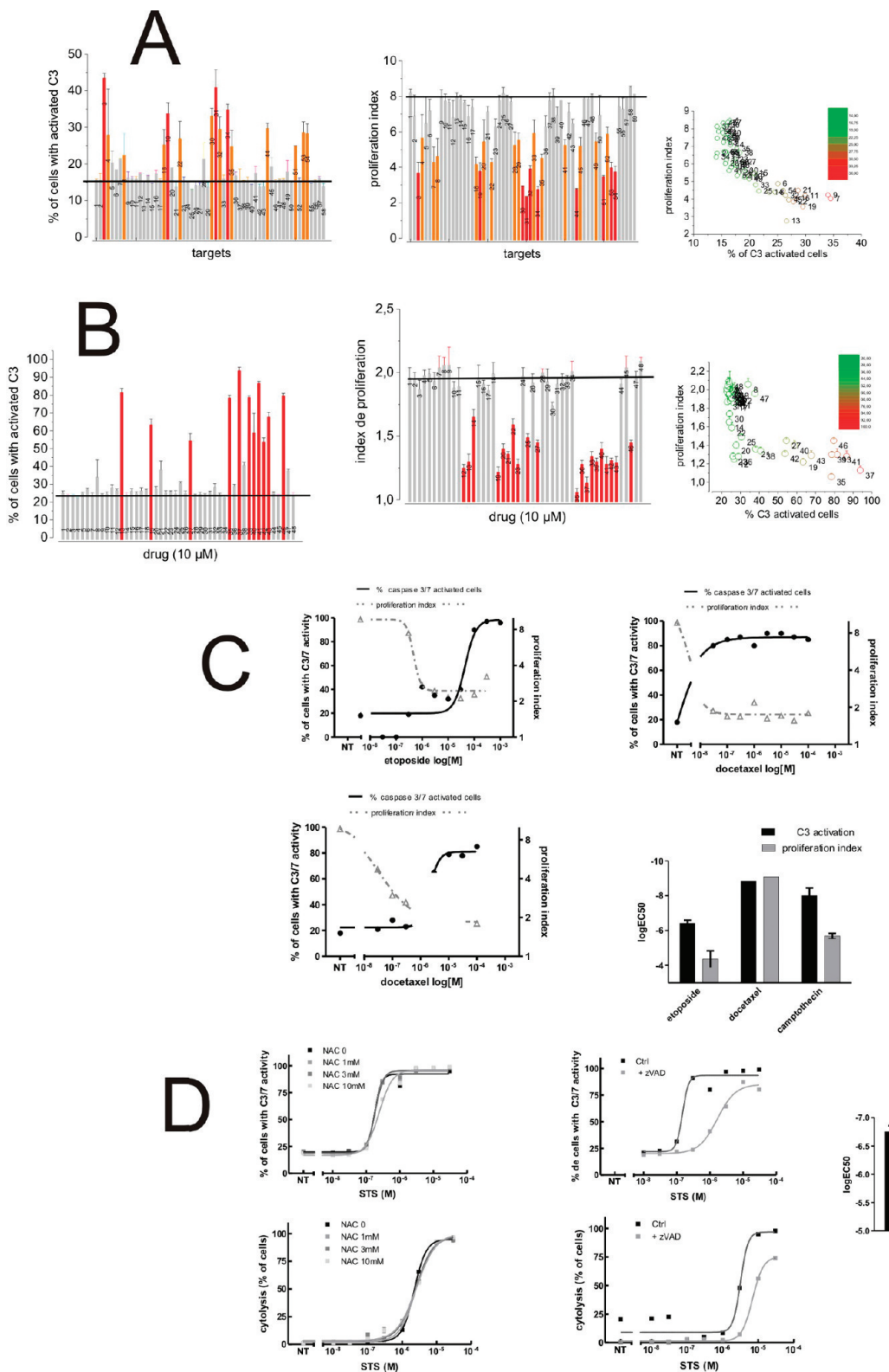


Figure 5. Multiplexed DAP assays as new tools for automated high content screening, high content analysis, and drug profiling. HeLa cell clone expressing mom-C3/C7 DAP was used to screen: (A) a library of 180 siRNAs targeting 60 kinases involved in cell cycle and (B) a library of 48 drugs (10 μ M 24 h). The screen was automated, and cytometry of caspase 3/7 was multiplexed with proliferation index. In each case, the results were represented on a biparametric plot (right-hand panels) to differentiate the pure antiproliferative/cytostatic hits, from those exhibiting combined cytostatic and proapoptotic features. (C) mom-C3/C7 DAP allowed one to characterize drugs in terms of EC50 and maximal efficacy. Dose response functions (eight points, triplicate) were generated for three reference anticancer drugs (24 h exposure) by multiplexing mom-C3/C7 DAP with proliferation (48 h drug exposure). Left panel shows the 1/EC50 values of each 2 parameter. (D) Multiplexing mom-C3/C7 DAP with EMA staining for simultaneous detection of DEVDase activity and cytosis. Left panel shows the 1/EC50 values of each 2 parameter.

3/7 activity (high EC50). This is in agreement with their mechanism of action: these drugs cause DNA damage that, second

to its extent, cause either proliferation arrest (low damage: p53-dependent onset of DNA repair) or switch the cell fate to death

(high damage: p53-dependent apoptosis). On the contrary, docetaxel exhibit a single EC50 characterizing both its cytostatic and proapoptotic activity. This is also in agreement with the notion that once bound to tubulin, docetaxel prevents cytokinesis and cell divisions, but at the same time, destabilizes the motor dynein complex and releases the proapoptotic protein Bim that triggers cell death.

The last example shows a multiplexed assay aimed at detecting simultaneously DEVDase activity and the loss of integrity of the plasma membrane, i.e., cytolysis. In this test, the detection of mom-C3/7 DAP was coupled to EMA, a cell impermeable fluorescent DNA intercalating agent that selectively enters cells with a compromised plasma membrane and that, once intercalated, increases its fluorescence yield and becomes photochemically fixable to DNA.²² Figure 5D shows dose-response functions obtained in this assay for STS in the presence of several doses of the antioxidant *N*-acetyl cysteine (NAC) or of the pan-caspase inhibitor zVAD-fmk. The results indicate that the EC50 for C3/7 activity and cytolysis are separated by one log and that zVAD-fmk is capable to shift both EC50s toward higher values, while NAC has no measurable impact on these effects of STS. This indicates that reactive oxygen species are not front players in the proapoptotic and cytolytic effects of STS.

CONCLUSION

In conclusion, we described here a new high content analytical strategy capable (i) of capturing molecular effects at the single cell level on large cellular populations and, thus, (ii) of obtaining a precise determination of quantitative parameters characterizing test conditions or compounds.

This new high content analytical strategy based on recombinant DAPs is capable of converting subcellular spatial signals into steady “all-or-none” fluorescence intensity responses. We have shown here that such DAPs-converted spatial signals can be acquired at the single cell level by high throughput flow cytometry, eliminating the need for image acquisition and analysis.

We validated different approaches of anchoring, based not strictly on transmembrane domains but also by lipid anchorage

(22) Riedy, M. C.; Muirhead, K. A.; Jensen, C. P.; Stewart, C. C. *Cytometry* **1991**, 12, 133–139.

and protein–protein or protein–DNA interactions. These different approaches to construct a DAP allowed (i) the detection of protease activities specifically segregated in the intracellular space, (ii) the evaluation of protease accessibility to subcellular domains, and (iii) the test of the topology/orientation at interfaces of candidate protease substrates. Moreover, simultaneously using several anchorage and different fluorescent proteins, we could multiplex assays targeting different proteases in the same cell.

Illustrated by the example of the caspase 3/7, the DAP technology appeared to be easily amenable to a fully automated multiplexed HCS standard meeting industrial requirements. C3/7 DAP offers a reliable method to evaluate intracellular DEVDase activity at the single cell level by flow cytometry and requires an extremely simple experimental protocol. This method is easily adaptable to a robotic platform for screening genetic or compound libraries on multiplexed assays coupling the detection of caspase 3 activity with other key cellular parameters. In its multiplexed version, our DAP technology allowed the simultaneous integration of several predictive parameters relevant for evaluating the therapeutic potential of new drug candidates or of new targets.

Work is in progress to define a series of predictive combinations of multiplexed DAP tests and of sets of pharmacological modulators applicable for the fine characterization of anticancer and neuroprotective drug candidates.

ACKNOWLEDGMENT

This work was supported by l'INSERM, la Région Aquitaine, l'ANR, l'ANVAR, Aquitaine Amorçage, l'Institut Bergonié, la Ligue Contre le Cancer, le Cancéropôle Grand Sud-Ouest, l'Association France Cancer, L'Université Franco-Italienne, and le Ministère de l'Enseignement Supérieur et de la Recherche.

SUPPORTING INFORMATION AVAILABLE

Additional information as noted in text. This material is available free of charge via the Internet at <http://pubs.acs.org>.

Received for review July 9, 2009. Accepted October 12, 2009.

AC9015227